Calculation of the temperature- and layer-thickness-dependent giant magnetoresistance in magnetic multilayers

1994 J. Phys.: Condens. Matter 6 21

(http://iopscience.iop.org/0953-8984/6/1/005)

J. Phys.: Condens. Matter 6 (1994) 21–32. Printed in the UK

Calculation of the temperature- and layer-thickness-dependent giant magnetoresistance in magnetic multilayers

Hideo Hasegawa
Department of Physics, Tokyo Gakugei University, Koganei, Tokyo 184, Japan

Received 26 August 1993, in final form 25 October 1993

Abstract. The temperature and layer-thickness dependence of the magnetoresitance (MR) in magnetic multilayers is discussed with the use of the finite-temperature band theory in which the effect of spin fluctuations is taken into account by means of the static functional-integral method. It is shown that our model calculation explains well the observed MR data of Fe/Cr multilayers recently reported by Gijs and Okada.

1. Introduction

The giant magnetoresistance (GMR) [1, 2] in magnetic multilayers is one of the most attractive phenomena in current solid-state physics. It has been theoretically studied with a semi-classical approach [3–7] based on the Boltzmann equation or a microscopic approach [8–12] based on the Kubo formula. Quite recently, the present author [12] has discussed the temperature dependence of the MR ratio with the use of the finite-temperature band theory [13–15], in which the effect of spin fluctuations at finite temperatures is taken into account by using the static functional-integral method combined with the coherent potential approximation (CPA) [16]. This approach has been shown to reconcile the duality of d electrons showing both the localized and itinerant character, and to be useful in understanding various finite-temperature properties of transition metals, alloys and multilayers [13–15]. In order to discuss the MR of magnetic multilayers at finite temperatures [12], we introduced randomness to multilayers and calculated their conductivity which is expressed in terms of the spin- and layer-dependent coherent potentials. It has been shown by our model calculation [12] that the calculated MR ratio explains the following features observed in many transition-metal multilayers [17–21] well: (i) the MR ratio is more significantly temperature dependent than the (average) layer moment, (ii) the temperature dependence of the MR ratio is more considerable in a multilayer with a larger ground-state MR ratio, and (iii) it is quasi-linear near the Curie temperature. We have adopted in [12] a very simple model where only the electron-scattering process between the adjacent magnetic layers is included. The purpose of the present paper is to generalize our model so as to take account of the the layer-thickness dependence of the MR ratio in order to enable a more realistic discussion of experimental data.

The paper is organized as follows: in section 2, we briefly review the finite-temperature band theory [13–15] and obtain the expression for the MR ratio including the layer-thickness dependence in magnetic layers. In section 3, our theory is applied to analyse the experimental data on Fe/Cr multilayers recently reported by Gijs and Okada [21]. Section 4 is devoted to the conclusion and discussion.

0953-8984/94/010021+12$07.50

2. Calculation method

2.1. The static spin-fluctuation theory

We adopt an N_f-layer thin film with the simple-cubic (001) interface. The layer parallel to the interface is assigned by the index n ($= 1 - N_f$). The film is assumed to consist of magnetic A and non-magnetic B atoms, which are randomly distributed in layer n with concentrations of x_n and y_n, respectively ($x_n + y_n = 1$). The film is described by the single-band Hubbard model as

$$H = \sum_s \sum_j \varepsilon_j c_{js}^\dagger c_{js} + \sum_s \sum_{jl} t_{jl} c_{js}^\dagger c_{ls} + \sum_j U_j n_{j\uparrow} n_{j\downarrow} \tag{1}$$

where c_{js} is an annihilation operator of an electron with spin $s(=\uparrow, \downarrow)$ on the lattice site j, $n_{js} = c_{js}^\dagger c_{js}$, and t_{jl} is the hopping integral. The atomic potential ε_j and the on-site interaction U_j are assumed to be given by ε^λ and U^λ when the lattice site j is occupied by a λ (= A, B) atom.

In order to study the finite-temperature properties of the magnetic film, we apply the functional-integral method within the static approximation to the model Hamiltonian given by (1). The partition function is given by [13]

$$Z = \int \prod_j \mathrm{d}\nu_j \prod_j \mathrm{d}\zeta_j \exp[-\beta(\phi_0 + \phi_1)] \tag{2}$$

with

$$\phi_0 = \tfrac{1}{4} \sum_j U_j (\nu_j^2 + \zeta_j^2) \tag{3}$$

$$\exp(-\beta\phi_1) = \mathrm{Tr} \exp(-\beta H_{\mathrm{eff}}) \tag{4}$$

$$H_{\mathrm{eff}} = \sum_s \sum_j \{[\varepsilon_j - (i/2) U_j \nu_j] n_j - \tfrac{1}{2} s U_j \zeta_j m_j\} + H_0'. \tag{5}$$

Here $n_j = n_{j\uparrow} + n_{j\downarrow}$, $m_j = n_{j\uparrow} - n_{j\downarrow}$, and H_0' denotes the second (hopping) term in (1). We can evaluate the partition function by calculating the partition function of the effective one-electron system given by H_{eff} including the random charge (ν_j) and exchange (ζ_j) fields with the Gaussian weight, $\exp(-\beta\phi_0)$. We take account of the charge field by the saddle-point approximation and the exchange field by the alloy-analogy approximation with the CPA. When the decoupling approximation is employed, the modified CPA equation is given by [13, 14]

$$x_n T_{ns}^{\mathrm{A}} + y_n T_{ns}^{\mathrm{B}} = 0 \tag{6}$$

with

$$T_{ns}^\lambda = \frac{\tilde{\varepsilon}_n^\lambda - s(U_n^\lambda/2)\langle\zeta_n^\lambda\rangle - \Sigma_{ns} + [(U_n^\lambda/2)^2 \langle(\zeta_n^\lambda)^2\rangle - (\Sigma_{ns} - \tilde{\varepsilon}_n^\lambda)^2] F_{ns}}{[1 - (\tilde{\varepsilon}_n^\lambda - \Sigma_{ns}) F_{ns}]^2 - (U_n^\lambda/2)^2 \langle(\zeta_n^\lambda)^2\rangle} \tag{7}$$

where $\tilde{\varepsilon}_n^\lambda = \varepsilon_n^\lambda + (U_n^\lambda/2)\langle N_n^\lambda\rangle$. The coherent potential Σ_{ns} for an s-spin electron on the layer n, is determined by (6) and (7), and is a function of ε_n^λ, $\langle\zeta_n^\lambda\rangle$, $\langle(\zeta_n^\lambda)^2\rangle$ and $\langle N_n^\lambda\rangle$ ($= -\mathrm{i}\langle\nu_n^\lambda\rangle$).

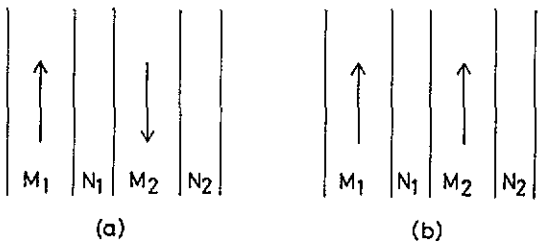

Figure 1. The adopted film consisting of magnetic (M_1 and M_2) and non-magnetic (N_1 and N_2) layers, their thicknesses being M and N, respectively. The moments on the magnetic layers align in the (a) antiferromagnetic (AF) and (b) ferromagnetic (F) configurations.

The self-consistent equations for $\langle\zeta_n^\lambda\rangle$, $\langle(\zeta_n^\lambda)^2\rangle$, and $\langle N_n^\lambda\rangle$ are given by

$$\langle\zeta_n^\lambda\rangle = \int d\zeta_j\, \zeta_j\, C_n^\lambda(\zeta_j) \tag{8}$$

$$\langle(\zeta_n^\lambda)^2\rangle = \int d\zeta_j\, \zeta_j^2\, C_n^\lambda(\zeta_j) \tag{9}$$

$$\langle N_n^\lambda\rangle = \int d\varepsilon\, f(\varepsilon) \sum_s (-1/\pi)\,\mathrm{Im}\, F_{ns}^\lambda(\varepsilon) \tag{10}$$

where $f(\varepsilon)$ is the Fermi-distribution function. We should note that $F_{ns}^\lambda(\varepsilon)$, the local Green function of an s-spin electron at a λ atom on layer n, and $C_n^\lambda(\zeta_j)$, the distribution of the potential of $(U_n^\lambda/2)\zeta_j$ when a λ atom occupies the layer n, are functions of the coherent potentials Σ_{ns}, which are functions of $\langle\zeta_n^\lambda\rangle$, $\langle(\zeta_n^\lambda)^2\rangle$, and $\langle N_n^\lambda\rangle$. Thus we have to simultaneously solve these quantities; details having been reported elsewhere [13–15]. Once these are determined, the average of the magnetic moment and its root-mean-square (RMS) values of a λ atom on the layer n are given by

$$\langle M_n^\lambda\rangle = \langle\zeta_n^\lambda\rangle \tag{11}$$

$$\langle(M_n^\lambda)^2\rangle^{1/2} = [\langle(\zeta_n^\lambda)^2\rangle - (2T/U_n^\lambda)]^{1/2}. \tag{12}$$

2.2. *Calculations of the MR ratio*

By using the CPA, we have shown [11] that the conductivity for currents parallel to the film layer is given by

$$\sigma = N_f^{-1} \sum_n \sigma_n \tag{13}$$

with

$$\sigma_n = (e/\hbar)^2 \pi \sum_s \sum_l \int d\varepsilon \left(-\frac{\partial f}{\partial \varepsilon}\right) \frac{\nu_s a_{nls}\, \tau_{nls}}{(\Delta_{ns} + \Delta_{ls})} \tag{14}$$

$$\tau_{nls} = \delta_{nl} + (1 - \delta_{nl}) \left(\frac{(\Delta_{ns} + \Delta_{ls})^2}{\left[(\Lambda_{ns} - \Lambda_{ls})^2 + (\Delta_{ns} + \Delta_{ls})^2\right]} \right) \tag{15}$$

which is valid within the Born approximation. In equations (13)–(15) $\Lambda_{ns} = \mathrm{Re}\ \Sigma_{ns}(\varepsilon)$, $\Delta_{ns} = |\,\mathrm{Im}\ \Sigma_{ns}(\varepsilon)\,|$, Σ_{ns} is the coherent potential of an s-spin electron on layer n, and a_{nls} and ν_s are specified by the electronic structure of the film (see equations (19) and (20) in [11]). We employ our conductivity formula in a semi-phenomenological way to discuss the layer-thickness dependence of the MR ratio.

We adopt a system consisting of magnetic (M_1, M_2) and non-magnetic (N_1, N_2) layers (see figure 1), whose thickness are M and N, respectively. Bulk scatterings are assumed to be important in these layers. When moments on the magnetic layers are in the antiferromagnetic (AF) configuration as shown in figure 1(a), the real and imaginary parts of the coherent potentials are given by [11]

$$\Lambda_{ns}^{AF} - i\Delta_{ns}^{AF} = \Lambda_s - i\Delta_s \qquad \text{for } n \in M_1 \tag{16}$$

$$\Lambda_{ns}^{AF} - i\Delta_{ns}^{AF} = \Lambda_{-s} - i\Delta_{-s} \qquad \text{for } n \in M_2 \tag{17}$$

$$\Lambda_{ns}^{AF} - i\Delta_{ns}^{AF} = \Lambda_0 - i\Delta_0 \qquad \text{for } n \in N_1, N_2. \tag{18}$$

The s-spin contribution to the conductivity is classified into five categories depending on whether n and m are in magnetic or non-magnetic layers. It is given by

$$\sigma_s^{AF} = \frac{2c_{MM}^{AF}}{\Delta_s + \Delta_{-s}} + \frac{c_{NN}^{AF}}{\Delta_0} + 4c_{MN}^{AF}\left(\frac{1}{\Delta_s + \Delta_0} + \frac{1}{\Delta_{-s} + \Delta_0}\right) + d_M^{AF}\left(\frac{1}{2\Delta_s} + \frac{1}{2\Delta_{-s}}\right) + \frac{d_N^{AF}}{\Delta_0} \tag{19}$$

where

$$c_{MM}^{AF} = N_f^{-1}(e/\hbar)^2\pi\nu \sum_{n\in M_1}\sum_{m\in M_2} a_{nm}\tau_{nm} \tag{20}$$

$$d_M^{AF} = N_f^{-1}(e/\hbar)^2\pi\nu \sum_{n\in M_1}\sum_{m\in M_1} a_{nm}\tau_{nm} \tag{21}$$

and c_{NN}^{AF}, c_{MN}^{AF}, and d_N^{AF} are given by similar expressions, the spin dependence in a_{nms} and τ_{nms} being neglected. In equation (19), subscripts MM, NN, and MN denote the contributions from the *interlayer* scatterings between magnetic layers, between non-magnetic layers, and between magnetic and non-magnetic layers, respectively. In contrast, the single subscript M (N) expresses the contribution from the *intralayer* scatterings within magnetic (non-magnetic) layers. We employed the $T = 0$ limit of equations (13)–(15) because the relevant temperature is much less than the Fermi energy.

In the ferromagnetic (F) configuration (figure 1(b)), on the other hand, the real and imaginary parts of the coherent potentials are given by [11]

$$\Lambda_{ns}^{F} - i\Delta_{ns}^{F} = \Lambda_s - i\Delta_s \qquad \text{for } n \in M_1, M_2 \tag{22}$$

$$\Lambda_{ns}^{F} - i\Delta_{ns}^{F} = \Lambda_0 - i\Delta_0 \qquad \text{for } n \in N_1, N_2. \tag{23}$$

We obtain the s-spin contribution to the conductivity given by

$$\sigma_s^{F} = \frac{c_{MM}^{F}}{\Delta_s} + \frac{c_{NN}^{F}}{\Delta_0} + \frac{8c_{MN}^{F}}{(\Delta_s + \Delta_0)} + \frac{d_M^{F}}{\Delta_s} + \frac{d_N^{F}}{\Delta_0}. \tag{24}$$

The total conductivities in the AF (σ^{AF}) and F (σ^{F}) configurations are obtained by summing both the up-spin and down-spin contributions (equation (14)). The difference between them is given by

$$\Delta\sigma = \sigma^{F} - \sigma^{AF} = c_{MM}^{F}\left(\frac{1}{\Delta_\uparrow} + \frac{1}{\Delta_\downarrow}\right) - 4c_{MM}^{AF}\left(\frac{1}{\Delta_\uparrow + \Delta_\downarrow}\right) \tag{25}$$

$$\Delta\sigma = \sigma^{F} - \sigma^{AF} = \frac{c_{MM}^{F}}{\Delta_0\alpha\beta(\alpha+\beta)}[(\alpha-\beta)^2 + 4b\alpha\beta] \tag{26}$$

where

$$\alpha = \Delta_\uparrow/\Delta_0 \qquad \beta = \Delta_\downarrow/\Delta_0 \qquad b = (c^{\mathrm{F}}_{\mathrm{MM}} - c^{\mathrm{AF}}_{\mathrm{MM}})/c^{\mathrm{F}}_{\mathrm{MM}} \tag{27}$$

with the configuration dependence of the coefficients being included only in c_{MM}. Equation (25) shows that the GMR arises mainly from the conductivity contribution from interlayer scatterings between the magnetic layers M_1 and M_2, because other contributions in equations (19) and (24) are cancelled out in calculating the difference $\Delta\sigma$.

By using equations (19), (24), and (26), the MR ratio $\Delta R/R$ is given by [11]

$$\frac{\Delta R}{R} \equiv \frac{(R^{\mathrm{AF}} - R^{\mathrm{F}})}{R^{\mathrm{F}}} = \frac{\Delta\sigma}{\sigma^{\mathrm{AF}}} = \left(\frac{(\alpha-\beta)^2}{4\alpha\beta} + \frac{b(\alpha+\beta)^2}{4\alpha\beta(1-b)}\right) X \tag{28}$$

with

$$X = \left[1 + g_0\frac{(\alpha+\beta)^2}{\alpha\beta} + g_1\left(\frac{N}{M}\right)(\alpha+\beta)\left(\frac{1}{\alpha+1} + \frac{1}{\beta+1}\right) + g_2\left(\frac{N}{M}\right)^2(\alpha+\beta)\right]^{-1}. \tag{29}$$

In equation (29) g_0, g_1, and g_2 are defined by

$$\frac{d_{\mathrm{M}}}{4c_{\mathrm{MM}}} = g_0 \qquad \frac{2c_{\mathrm{MN}}}{c_{\mathrm{MM}}} = g_1\left(\frac{N}{M}\right) \qquad \left(\frac{c_{\mathrm{NN}} + d_{\mathrm{N}}}{2c_{\mathrm{MM}}}\right) = g_2\left(\frac{N}{M}\right)^2 \tag{30}$$

which come from the following relations:

$$c_{\mathrm{MN}} \propto MN \qquad c_{\mathrm{NN}} \propto d_{\mathrm{N}} \propto N^2 \qquad c_{\mathrm{MM}} \propto d_{\mathrm{M}} \propto M^2. \tag{31}$$

The first and second terms in equation (28) denote the contributions from the *short-circuit* and *valve* effects, respectively [11, 12]. The short-circuit effect has been discussed previously [3–9]. It has been shown [11, 12] that the valve effect works to enhance the GMR [11]. By using a phenomenological approach, Edwards *et al* [6] obtained a result similar to the first term of equation (28) although their discussion is limited to the $T = 0$ case. When we set $X = 1$ in equation (28), it yields

$$\frac{\Delta R}{R} = \frac{(a-1)^2}{4a} + \frac{b(a+1)^2}{4a(1-b)} \qquad (a = \alpha/\beta). \tag{32}$$

This is the result obtained in [12], where only the contribution from the interlayer scattering between the magnetic layers is taken into account.

Now we consider the coherent potentials of the film, which can be evaluated by solving equations (6)–(10). The real and imaginary parts of the coherent potential in the magnetic (M_1 or M_2) layer are given within the Born approximation by [12]

$$\Lambda_s = x\left[\tilde{\varepsilon}^{\mathrm{A}} - s\left(\frac{U^{\mathrm{A}}}{2}\right)\langle M^{\mathrm{A}}\rangle\right] + y\,\tilde{\varepsilon}^{\mathrm{B}} \tag{33}$$

$$\Delta_s = \Delta_s^{\mathrm{r}} + \Delta^{\mathrm{s}} + \Delta^{\mathrm{p}} \tag{34}$$

with

$$\Delta_s^{\mathrm{r}} = \pi\rho x\, y\left[\tilde{\varepsilon}^{\mathrm{A}} - \tilde{\varepsilon}^{\mathrm{B}} - s\left(\frac{U^{\mathrm{A}}}{2}\right)\langle M^{\mathrm{A}}\rangle\right]^2 \tag{35}$$

$$\Delta^{\mathrm{s}} = \pi\rho x\left(\frac{U^{\mathrm{A}}}{2}\right)^2[\langle (M^{\mathrm{A}})^2\rangle - \langle M^{\mathrm{A}}\rangle^2] \tag{36}$$

where $\tilde{\varepsilon}^{\lambda} = \varepsilon^{\lambda} + (U^{\lambda}/2)\langle N^{\lambda}\rangle$ (λ = A, B), $U^{B} = 0$ for a non-magnetic B atom, and ρ is the density of states at the Fermi level. The first term Δ_s^r in equation (34) arises from the scattering due to random Hartree–Fock potentials for an s-spin electron; the second term (Δ^s) originates from the effect of spin fluctuations; the third term Δ^p arises from the electron–phonon interaction, whose explicit form is not necessary here. On the other hand, the real and imaginary parts of the coherent potential in the non-magnetic (N_1 or N_2) layer are assumed to be given by

$$\Lambda_0 = 0 \tag{37}$$

$$\Delta_0 = \Delta_0^r + \Delta_0^p. \tag{38}$$

Equation (37) defines the origin of the energy scale, and the first and second terms in equation (38) denote the contributions from random potentials and phonons, respectively.

For a simplicity of our model calculation, we neglect the phonon contributions given by Δ^p and Δ_0^p in equations (34) and (38); related discussion will be given in section 4. Using equations (27), (34), and (38), we obtain α, β, and b given by

$$\alpha = \alpha^r + \alpha^s = A[B + m(T)]^2 + A\,y^{-1}[\mu(T)^2 - m(T)^2] \tag{39}$$

$$\beta = \beta^r + \beta^s = A[B - m(T)]^2 + A\,y^{-1}[\mu(T)^2 - m(T)^2] \tag{40}$$

$$b = \frac{m(T)^2}{m(T)^2 + C^{-1}\{y[B^2 + m(T)^2] + [\mu(T)^2 - m(T)^2]\}^2} \tag{41}$$

with

$$m(T) = \langle M^A\rangle/M_0 \tag{42}$$

$$\mu(T) = \sqrt{\langle (M^A)^2\rangle}/M_0 \tag{43}$$

$$A = \pi\rho x y (U^A M_0/2)^2/\Delta_0 \tag{44}$$

$$B = (2/U^A M_0)(\tilde{\varepsilon}_B - \tilde{\varepsilon}_A) \tag{45}$$

$$C = (2/\pi\rho\, U^A M_0)^2 \tag{46}$$

where M_0 is the ground-state magnetic moment.

At $T = 0$ K where $m(0) = \mu(0) = 1$, equations (39)–(41) become

$$\alpha_0 = \alpha(T = 0) = A(B + 1)^2 \tag{47}$$

$$\beta_0 = \beta(T = 0) = A(B - 1)^2 \tag{48}$$

$$b_0 = b(T = 0) = 1/[1 + C^{-1}\,y^2\,(B^2 + 1)^2] \tag{49}$$

from which the coefficients A, B and C are expressed in terms of α_0, β_0, b_0, and y as

$$A = (\sqrt{\alpha_0} - \sqrt{\beta_0})^2/4 \tag{50}$$

$$B = (\sqrt{\alpha_0} + \sqrt{\beta_0})/(\sqrt{\alpha_0} - \sqrt{\beta_0}) \tag{51}$$

$$C = [b_0/(1 - b_0)]\,y^2\,(B^2 + 1)^2. \tag{52}$$

The normalized magnetic moment $m(T)$ and its RMS value $\mu(T)$ are in principle calculated by using equations (11) and (12) in the finite-temperature band theory [13, 14].

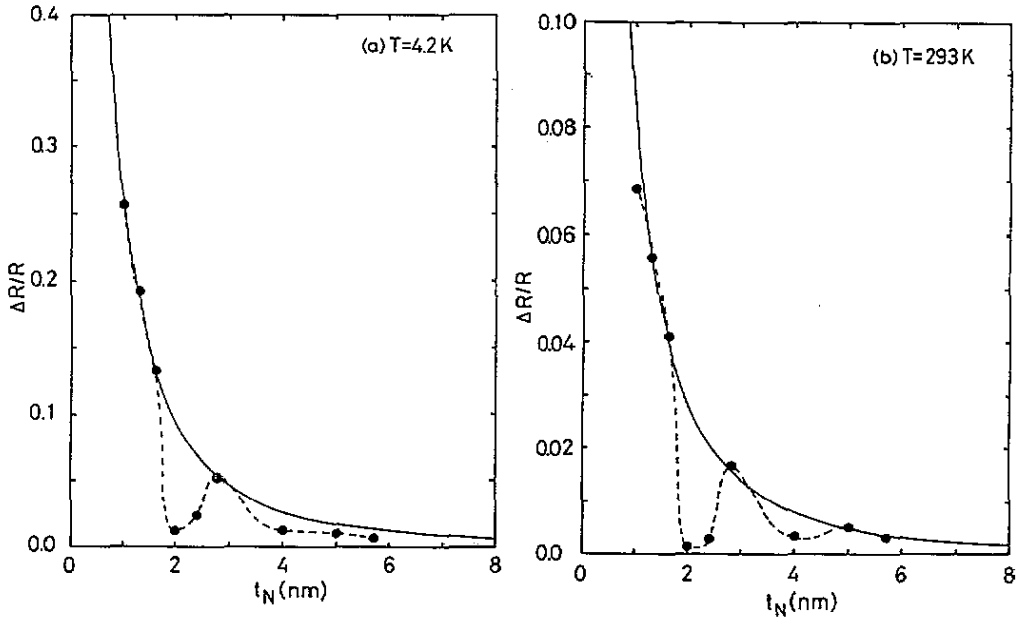

Figure 2. The dependence of the MR ratio $\Delta R/R$ on the thickness t_N (nm), of the non-magnetic layer of (3 nm Fe + t_N Cr) multilayers at (a) T = 4.2 K and (b) T = 293 K. Solid curves show the calculated results and circles express the observed data [21], the dashed curve being a guide to the eye.

Here, however, we adopt simple, analytic expressions of $m(T)$ and $\mu(T)$ for our model calculation given by [12]

$$m(T) = \sqrt{1 - (T/T_C)^2} \qquad \mu(T) = 1. \tag{53}$$

Now we may calculate the MR ratio $\Delta R/R$ as functions of T/T_C and N/M with the use of equations (28), (29), (39)–(41) and (50)–(53), when we treat α_0, β_0, b_0, g_0, g_1, g_2, and y as input parameters. Our strategy for calculating the temperature- and layer-thickness-dependent MR ratio is as follows: we determine a set of the six parameters, α_0, β_0, b_0, g_0, g_1, and g_2, so as to reproduce the N/M dependence of the *ground-state* MR ratio. Note that α_0, β_0, and b_0 are ground-state values of the relevant parameters and that g_0, g_1, and g_2 given by equation (30) are determined by the structure of the multilayer. Then, fixing the six parameters thus determined, we calculate the *finite-temperature* MR ratio for a chosen y parameter. We will demonstrate the feasibility of our theory by showing a model calculation in the next section.

3. Model calculations

In order to make our discussion concrete, we consider, as an example, the systematic, experimental data for Fe/Cr layers recently reported by Gijs and Okada [21], which are reproduced in figures 2 and 3. Circles in figures 2(a) and (b) show their data on the MR ratio $\Delta R/R$ at T = 4.2 K and 293 K, respectively, as a function of the thickness t_N (nm), of the non-magnetic (Cr) layer, in (3 nm Fe + t_N Cr) multilayers. The temperature dependence of the observed MR ratio is shown in figure 3 where symbols denote the data for various t_N values.

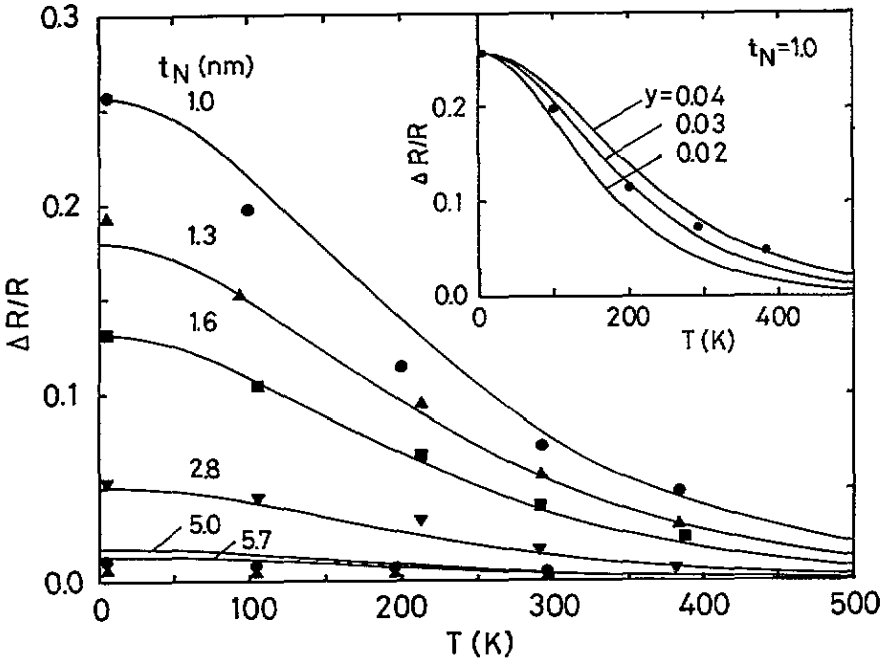

Figure 3. The temperature dependence of the MR ratio $\Delta R/R$ for various t_N. Solid curves denote the results calculated with $y = 0.04$ and symbols the observed data [21]. The inset shows the $\Delta R/R$ calculated for $t_N = 1.0$ nm by changing the y value in the model.

Firstly we consider the case of $T = 4.2$ K shown in figure 2(a). It should be noted that the oscillation in the observed MR ratio arises because the MR is measured only for the t_N values for which the Fe moments are coupled antiferromagnetically [1, 2]. It is then only meaningful to compare the calculated and observed results with the envelope of the observed $\Delta R/R$. The solid curve in figure 2(a) shows the result calculated by using equations (28), (29), (39)–(41) and (50)–(52) with $\alpha_0 = 6$, $\beta_0 = 1$ [6], $b_0 = 0$, $g_0 = 0$, $g_1 = 0.64$, and $g_2 = 2.68$. These parameters are chosen such that we have a good fit to the envelope of the observed t_N dependence of $\Delta R/R$ [22].

Next we consider the MR ratio at $T = 293$ K shown in figure 2(b). We assume the Curie temperature of the multilayer to be $T_C = 1000$ K because the thickness of the Fe layers of the Fe/Cr multilayers adopted [21] is sufficiently thick to sustain the Curie temperature of bulk Fe. The solid curve in figure 2(b) shows the t_N-dependent $\Delta R/R$ at $T = 293$ K calculated with $y = 0.04$. The calculation reproduces the observed t_N dependence of the MR ratio well.

Similar calculations are performed by changing the temperature. Solid curves in figure 3 show the calculated $\Delta R/R$ as a function of T and t_N. Our calculation explains the behaviour of the observed data fairly well. For the case of $t_N = 1.0$ nm, however, the agreement between the calculated and observed results is not satisfactory, so we repeated our calculation for this case by changing the y value, the result of which is shown in the inset. When the y value is decreased, the fit to the observed data becomes better below 200 K, but worse above 300 K. This disagreement may be due to the fact that the interface scattering, neglected in our calculation, may be important in thin Cr layers. It has been shown by the microscopic calculation for Fe/Cr multilayers [23] that spin fluctuations at the

interface are more significant than those in the bulk. We would expect that the temperature dependence of the MR ratio becomes more considerable than that of our calculation because spin fluctuations at interface layers work to reduce the MR ratio further, particularly at low temperatures.

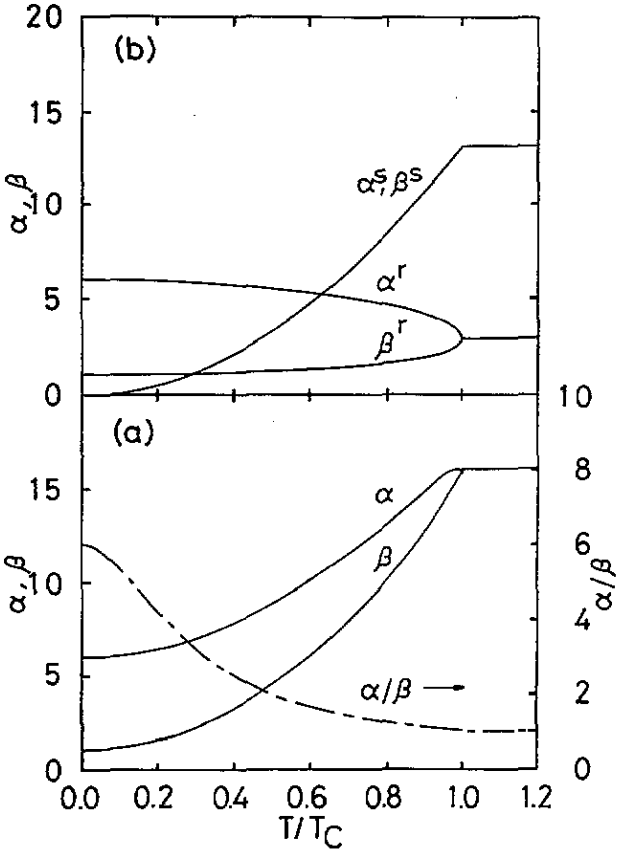

Figure 4. (a) The temperature dependence of α, β, and α/β. (b) Their decomposition: $\alpha = \alpha^r + \alpha^s$ and $\beta = \beta^r + \beta^s$ (see equations (39) and (40)).

In order to study the temperature dependence of the MR ratio in more detail, we show, in figure 4(a), α and β as a function of the temperature. Although $\alpha = 6$ and $\beta = 1$ at $T = 0$, they increase up to $\alpha = \beta = 16.1$ at $T \geqslant T_C$ because of the contribution from spin fluctuations. Then the ratio α/β changes from six at $T = 0$ to unity at $T \geqslant T_C$. Figure 4(b) shows the decomposition of α and β to $\alpha = \alpha^r + \alpha^s$ and $\beta = \beta^r + \beta^s$ where α^r and β^r denote the contributions from the random potentials whereas α^s (= β^s) denote those from spin fluctuations (see equations (39) and (40)). Figure 5(a) shows the calculated temperature dependence of the resistivity normalized by R^C, the resistivity at $T = T_C$, for various t_N values in the AF and F configurations in the temperature range of $0.0 \leqslant T/T_C \leqslant 1.0$. We should remark that the R^C value is much decreased when t_N becomes larger. The relevant GMR ratio is plotted in figure 5(b), where the inset shows the enlarged plot for $0.6 \leqslant T/T_C \leqslant 1.0$.

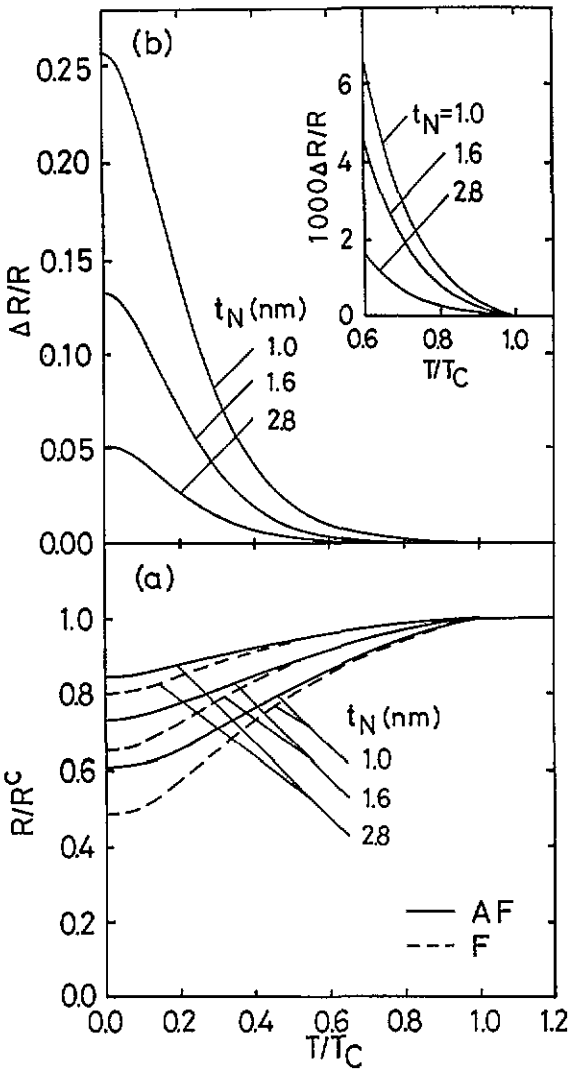

Figure 5. (a) The temperature dependence of the resistivity R/R^C in AF (solid curves) and F (dashed curves) configurations for various t_N, R^C being the resistivity at $T = T_C$. (b) The temperature dependence of the MR ratio $\Delta R/R$, the inset showing the enlarged plot at $0.6 \leqslant T/T_C \leqslant 1.0$.

The temperature dependence of the MR ratio normalized by its ground-state value, $(\Delta R/R)_0$, is plotted in figure 6 for various t_N values. Note that in the case of $t_N = 0.0$, the MR ratio is given by equation (32). It is interesting to note that this normalized MR ratio is almost independent of the t_N value, which arises from the fact that the factor X given by equation (29) has little temperature dependence. This implies that the temperature dependence of the MR ratio is predominantly determined by that of the ratio $a = \alpha/\beta$.

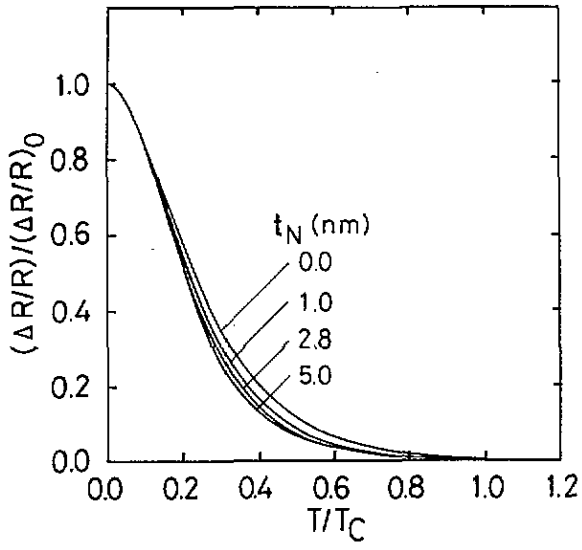

Figure 6. The temperature dependence of the MR ratio normalized by its ground-state value, $(\Delta R/R)_0$, for various t_N (see text).

4. Conclusion and discussion

We have discussed the temperature- and layer-thickness-dependent MR ratio in magnetic layers by generalizing the conductivity expression obtained previously [11, 12]. We have included contributions from the random exchange potentials and spin fluctuations, which are considered to be the main scattering mechanisms yielding the resistivity in transition-metal multilayers. In what follows we briefly examine the effect of the electron–phonon interaction, which is neglected in our model calculation. When contributions Δ^p and Δ_0^p from the electron–phonon interaction in equations (34) and (38) are taken into account, $\alpha(= \Delta_\uparrow/\Delta_0)$ and $\beta(= \Delta_\downarrow/\Delta_0)$ are expected to have an additional temperature dependence besides those arising from spin fluctuations and random exchange potentials. Even in this case, however, the ratio $a = \alpha/\beta$ still has the bound values of six at $T = 0$ and unity at $T \geqslant T_C$ [24], as was shown in figure 4(a), although the temperature dependence of a at $0 < T/T_C < 1$ may be slightly modified from that calculated without phonon contributions. This justifies, to some extent, our approximation neglecting the contribution from the electron–phonon interaction, because the temperature dependence of the MR ratio is mainly determined by that of the ratio $a = \alpha/\beta$, as was shown at the end of section 3. The essential features of the temperature and Cr-thickness dependence of the MR ratio of Fe/Cr multilayers Gijs and Okada [21] recently reported are fairly well explained by our model calculation, in which the spin-dependent bulk scattering is assumed to be predominant. For a better understanding of the observed data, it would be necessary to also include the interface scattering and to investigate the respective roles of the interface and bulk scatterings, although the MR in Fe/Cr systems is conventionally considered to arise from the interface scattering [25]. In the present study, our finite-temperature band theory [12–15] has been semi-phenomenologically employed. We are now considerating performing a *microscopic* calculation of the MR at finite temperatures, introducing randomness on the interface and/or bulk layers into the model employed in [23].

Acknowledgment

This work is partly supported by a Grant-in-Aid for Scientific Research on Priority Areas from the Japanese Ministry of Education, Science and Culture.

References

[1] Baibich M, Broto J M, Fert A, Nyuyen Van Dau N, Petroff F, Eitenne P, Creuzet G, Friedrich A and Chazelas J 1988 *Phys. Rev. Lett.* **61** 2472
Binash G, Grünberg P, Saurenbach F and Zinn W 1990 *Phys. Rev.* B **39** 4828

[2] Parkin S S P, More N and Roche K P 1990 *Phys. Rev. Lett.* **64** 2304
Unguris J, Celotta R J and Pierce D T 1991 *Phys. Rev. Lett.* **67** 140
Purcell S T, Folkers W, Johnson M T, McGee N W E, Jager K, an de Stegge J, Zeper W B, Hoving W and Grünberg P 1991 *Phys. Rev. Lett.* **67** 903

[3] Camley R E and Barnas J 1989 *Phys. Rev. Lett.* **63** 664

[4] Barthelemy A and Fert A 1991 *Phys. Rev.* B **43** 13 124

[5] Johnson B L and Camley R E 1991 *Phys. Rev.* B **44** 9997

[6] Edwards D M, Mathon J and Muniz R B 1991 *IEEE Trans. Magn.* **27** 3548

[7] Hood R Q and Falicov L M 1992 *Phys. Rev.* B **46** 8287

[8] Levy P M, Zhang S and Fert A 1990 *Phys. Rev. Lett.* **65** 1643

[9] Inoue J, Oguri A and Maekawa S 1991 *J. Phys. Soc. Japan* **60** 376
Inoue J, Itoh H and Maekawa S 1992 *J. Phys. Soc. Japan* **61** 1149

[10] Okiji A, Nakanishi H, Sakata K and Kasai H 1992 *Japan. J. Appl. Phys.* **31** L706

[11] Hasegawa H 1993 *Phys. Rev.* B **47** 15073; equation (10) in [11] should be corrected to $A_{nm}^{(l)} = C_{mn}(D_l)\prod_{j(\neq l)}(D_l - D_j)^{-1}$.

[12] Hasegawa H 1993 *Phys. Rev.* B **47** 15080

[13] Hasegawa H 1979 *J. Phys. Soc. Japan* **46** 1504; 1980 *J. Phys. Soc. Japan* **49** 178

[14] Hasegawa H 1981 *J. Phys. Soc. Japan* **50** 802

[15] Soven P 1967 *Phys. Rev.* **156** 809
Velicky B 1969 *Phys. Rev.* **184** 614

[16] Hasegawa H and Herman F 1988 *Phys. Rev.* B **38** 4863

[17] Chaiken A, Tritt T M, Gillespie D J, Krebs J J, Lubitz P, Hanrford M Z and Prinz G A 1991 *J. Appl. Phys.* **69** 4798

[18] Dieny B, Speriosu V S and Metin S 1991 *Europhys. Lett.* **15** 227
Dieny B, Humbert P, Speriosu V S, Metin S, Gurney B A, Baumgart P and Lefakis H 1992 *Phys. Rev.* B **45** 806

[19] Yamamoto H, Okuyama T, Dohnomae H and Shinjo T 1991 *J. Magn. Magn. Mater.* **99** 243

[20] Mattson J E, Brubaker M E, Sowers C H, Conover M, Qiu Z and Bader S D 1991 *Phys. Rev.* B **44** 9378

[21] Gijs M A M and Okada M 1992 *Phys. Rev.* B **46** 2908; 1992 *J. Magn. Magn. Mater.* **113** 105; experimental data on the MR ratio, which are originally presented by $(R^{AF} - R^{R})/R^{AF}$ in [21] are recalculated to show $\Delta R/R \equiv (R^{AF} - R^{R})/R^{F}$ in our figures 2 and 3.

[22] These parameters are given as one of the conceivable sets of the six parameters, which are not uniquely determined from experimental data. Although the t_N dependence of the MR ratio is governed by g_0, g_1, and g_2, its temperature dependence is predominantly determined by the ratio α/β, as will be shown at the end of section 3.

[23] Hasegawa H 1993 *J. Magn. Magn. Mater.* **126** 384

[24] We can show that $a = 6$ because of the absence of the phonon contribution at $T = 0$ K, and that $a = 1$ in the paramagnetic state where there is no spin dependence in α and β regardless of the phonon contribution.

[25] Petroff F, Barthelemy A, Hamzic A, Fert A, Etienne P, Lequien S and Creuzet G 1991 *J. Magn. Magn. Mater.* **93** 95
Baumgart P, Gurney B A, Wilhoit D R, Thao Nyuyen, Dieny B, and Speriousu V S 1991 *J. Appl. Phys.* **69** 4792
Dieny 1992 *J. Phys.: Condens. Matter* **4** 8009
Obi Y, Takanashi K, Mitani Y, Tsuda N and Fujimori H 1992 *J. Magn. Magn. Mater.* **104-107** 1747
Fullerton E E, Kelly D M, Guimpel J, Schuller I K and Bruynseaede Y 1992 *Phys. Rev. Lett.* **68** 859
Jacob M, Reiss G, Bruckl H and Hoffmann H 1992 *Phys. Rev.* B **46** 11 208
Parkin S S P and York B R 1993 *Appl. Phys. Lett.* **62** 1842; see also [3], [5], [7] and [21].